An efficient base and H₂O₂ free protocol for the synthesis of phenols in water and oxygen using spinel CuFe₂O₄ magnetic nanoparticles

Rituparna Chutia & Bolin Chetia

View supplementary material 🗗

Published online: 10 Aug 2020.

Submit your article to this journal 🗗

Article views: 6

View related articles 🗗

View Crossmark data 🗗

Check for updates

An efficient base and H_2O_2 free protocol for the synthesis of phenols in water and oxygen using spinel $CuFe_2O_4$ magnetic nanoparticles

Rituparna Chutia and Bolin Chetia

Department of Chemistry, Dibrugarh University, Dibrugarh, Assam, India

ABSTRACT

An efficient base and H_2O_2 free protocol was used for the synthesis of phenols from boronic acids using biogenic $CuFe_2O_4$ magnetic nanoparticles as catalyst at room temperature in water and oxygen. The catalyst was prepared using the flowers of *Lantana camara*. The size of the nanoparticles was 4.27 nm. Base free and ligand free protocol, less time, excellent yields, room temperature, biogenic synthesis of the catalyst, use of O_2 as an environmentally friendly oxidant are the advantages of the present protocol. The recyclability of the catalyst was for 5 cycles without loss of magnetic property or catalytic activity.
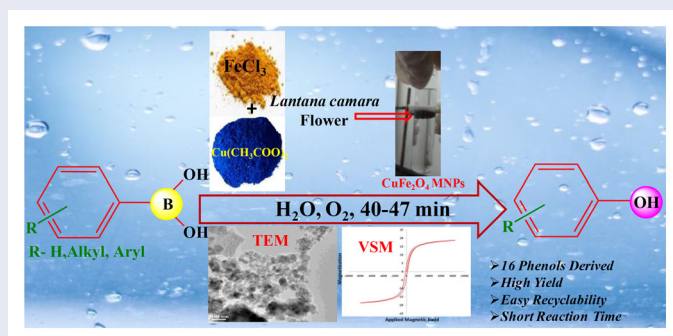
1. Introduction

Phenol and its derivatives have received attention as it is the major constituent of various pharmaceuticals [1, 2], polymers [3], natural antioxidants [4], *etc*. They also play an important role in the prevention and treatment of various diseases. Phenolic compounds obtained from natural products exhibit wide biological activities including anticancer, anti-allergic, antioxidant [5–8], *etc*. Given the importance of phenols, a wide range of reactions have been used to prepare them. Phenols are generally

---

synthesized [9] by nucleophilic substitution of an aryl halide with catalyst like palladium, copper, *etc.* But these reactions suffer from several disadvantages like poor functional group compatibility, harsh reaction conditions, and less substrate scope. Recently various transformations of boronic acids, oxidative C-B bond cleavage and oxidative hydroxylation (*ipso*-hydroxylation) of aryl boronic acids are used for preparation of phenols. Literature cited *ipso*-hydroxylation of boronic acids to phenols using various methods with different catalysts and reaction conditions. Various oxidants were cited in literature for the synthesis of phenols and its derivatives, which includes ozone [10], m-chloroperoxybenzoic acid [11], sodium perborate [12], hydroxylamine [13], tert-butyl hydroperoxide [14], N-oxide [15], H_2O_2 [16–19], *etc.*

The desire for eco-friendly, greener, simple and easy reaction methodologies [20] has led to enormous advancement [21]. Compared to the other oxidants and reaction conditions, the use of molecular oxygen and air have been well established as environmentally friendly and inexpensive oxidants for oxidations reactions [22, 23]. Wang *et al.* [24] used $CuSO_4$-catalyzed aerobic oxidative hydroxylation of arylboronic acid to phenols. Yang *et al.* [25] synthesized $CuFe_2O_4$ magnetic nanocatalyst for the *ipso*-hydroxylation of aryl boronic acid using air and oxygen. The easy recyclability of the catalyst from the reaction media with the use of an external magnet added as an advantage compared to previously reported methods but the reaction proceeded with the addition of base and took about 24 h for completion. A temperature of 40–50 °C was also favorable for the reaction. Thus a mild protocol for the synthesis of phenols was necessary.

Looking at the immense applications of phenols we have also performed oxidative-hydroxylation (*ipso*-hydroxylation) previously using $CuFe_2O_4$ magnetic nanoparticles (MNPs) which were prepared by co-precipitation method [26]. The use of $NaBH_4$ as a reducing reagent in the preparation of the catalyst and the use of H_2O_2 as an oxidizing agent in the process of *ipso*-hydroxylation prevent it from being as a green protocol. Thus, we have modified our method and report herein a green pathway for the synthesis of the catalyst as well as for *ipso*-hydroxylation. We obtained nanoparticles with smaller size and better catalytic activity in comparison to earlier reported catalysts.

We have synthesized here biogenic $CuFe_2O_4$ MNPs using flowers of *Lanatana camara* under mild reaction conditions. The nanoparticles are then used for *ipso*-hydroxylation of aryl boronic acids to phenols at room temperature within a very short reaction time without the use of a base. The presence of different phenolic compounds in the flowers might be mainly responsible for efficient *ipso*-hydroxylation with excellent yields.

Lantana camara is an aromatic perennial shrub with a wide range of flower color *viz.* red, white, yellow, pink, violet found in many countries of the world. It is mainly used as an ornamental plant in hedges of public and private gardens. In the present study the flower extract of *Lantana camara* is used as a reducing agent for the synthesis of $CuFe_2O_4$ MNPs. This plant also has medicinal value [27, 28], a rich source of many bioactive molecules, containing many triterpenes, steroids and flavonoids [29, 30]. The flower extracts mainly contained higher levels of carbohydrates compared to the leaves. Moreover, ontogenic variation in secondary metabolites such as phenolics, anthocyanins, and proanthocyanidins in *Lantana camara* have also been reported [31].

Table 1. Comparison with other reported $CuFe_2O_4$ nanocatalysts prepared using plants.

Plant	Method	Reaction temperature (°C)/time (h)	Annealing temp (°C)/time (h)	Size (nm)	Reference
Hibiscus rosa sinensis	Conventional combustion method	rt, several hours	1100, 4	50-200	[32]
Neem	Biogenic	rt, 1	800, 4	19.7	[33]
Jatropha oil	Green combustion route	rt, several hours	500, 5 min	12	[34]
Tragacanth gum	Sol-gel method	75, 12	600, 4	14	[35]
Lantana camara flowers	Biogenic	rt, 1	300, 2	4.27	This work

The presence of high phenolic content in this plant might be mainly responsible for its reducing character. Thus, owing to importance of this plant we tried to use it for the preparation of $CuFe_2O_4$ MNPs.

2. Experimental

2.1. General information

All reagents of analytical grade were used without purification. Ferric chloride ($FeCl_3$), cupric acetate monohydrate [$(CH_3 \cdot COO)_2Cu \cdot H_2O$], sodium hydroxide (NaOH), ethanol, diethylether, anhydrous Na_2SO_4 and different arylboronic acids were purchased from commercial suppliers. By using thin layer chromatography on silica gel plates ($60 F_{254}$) the progress of the reaction was monitored. The products were confirmed by ^1H NMR and ^{13}C NMR spectroscopy.

2.2. Preparation of the catalyst

According to a literature survey, $CuFe_2O_4$ MNPs have been synthesized using different plants by many researchers [32–35]. The prepared catalyst was compared with other reported $CuFe_2O_4$ catalyst synthesized by using different plant extracts and it was found that our catalyst required less annealing temperature and was cost efficient (Table 1).

For the preparation of the catalyst we used the flowers of *Lantana camara* which were collected from the Sivasagar District of Assam, India. The nanocatalyst was prepared in a similar manner to our previously reported work [36, 37].

3. Results and discussion

3.1. Characterization of the catalyst

The biogenic $CuFe_2O_4$ MNPs were characterized by XRD diffraction (Figure 1). The sharp diffraction peaks from the XRD analysis reveal the crystalline nature of the MNPs. The diffraction peaks at $2\theta = 24.20°$, $30.25°$, $31.66°$, $33.19°$, $35.66°$, $38.74°$, $40.90°$, $45.39°$, $49.51°$, $54.1°$, $56.51°$, $57.62°$, $62.47°$ and $64.04°$ correspond to planes (111), (202), (220), (113), (311), (222), (004), (400), (331), (422), (333), (511), (404) and (440), respectively (JCPDS 34-0425). The diffraction peaks with the Miller indices suggest inverse tetragonal spinel structure of the MNPs. Some additional peaks showing
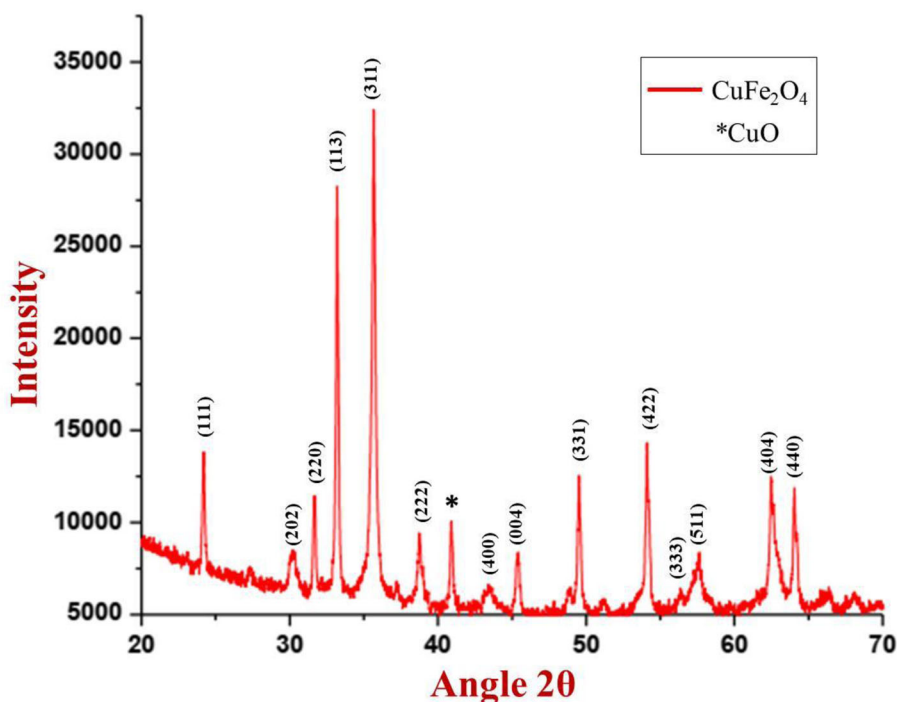
Figure 1. Powder XRD pattern of the synthesized CuFe$_2$O$_4$ MNPs.

traces of CuO were also noticed which corresponds to JCPDS card No. 48-1548. From the XRD analysis, distance between the planes (d) can also be found which is given by using the Bragg's equation (1):

$$\lambda = 2d\sin\theta \tag{1}$$

where λ is the wavelength of X-ray and θ represents the Bragg's reflection angle. The value of "d" calculated from the above equation was 0.249 nm.

From the SEM images (Figure S1) monodispersity of the nanocrystals was observed. There was slight aggregation of the nanoparticles as seen from the SEM images. The Energy Dispersive X-ray (EDX) spectrum (Figure 2) shows the presence of copper, iron and oxygen in the nanoparticle. As detected from the EDX analysis the maximum intensity was found with Cu ion with the second and third intensity peaks of Fe and O, respectively. The spectrum provided the final confirmation of CuFe$_2$O$_4$ nanoparticles. The inset clearly shows the atomic and weight percentage of CuFe$_2$O$_4$ with corresponding stoichiometry values of existing Fe, Cu and O elements.

From the TEM image (Figure 3(a)) the size and morphology of the nanoparticles were determined. The selected area electron diffraction (SAED) pattern of the CuFe$_2$O$_4$ MNPs showed bright circles which indicated the polycrystalline nature of the nanoparticles (Figure 3(b)). Moreover, the crystallographic planes viz., (111), (202), (220), (113), (311), (222), (004), (400), (331), (422), (333), (511), (404) and (440) were clearly indexed in this SAED pattern. The HR-TEM image (Figure 3(c)) shows the fringe separations of 4.09 A° and 2.79 A°, in agreement with (111) and (311) planes; this also confirmed the polycrystalline nature of the synthesized MNPs as the orientations of planes are in
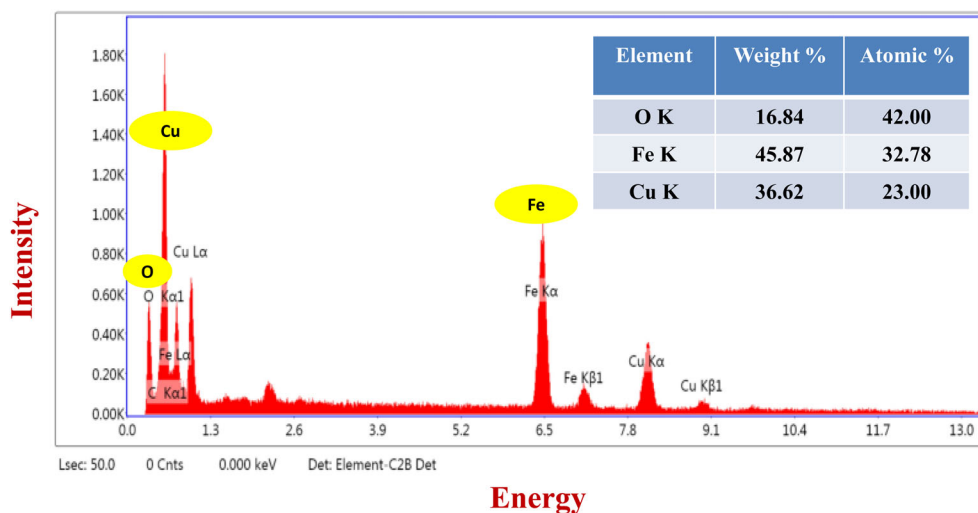
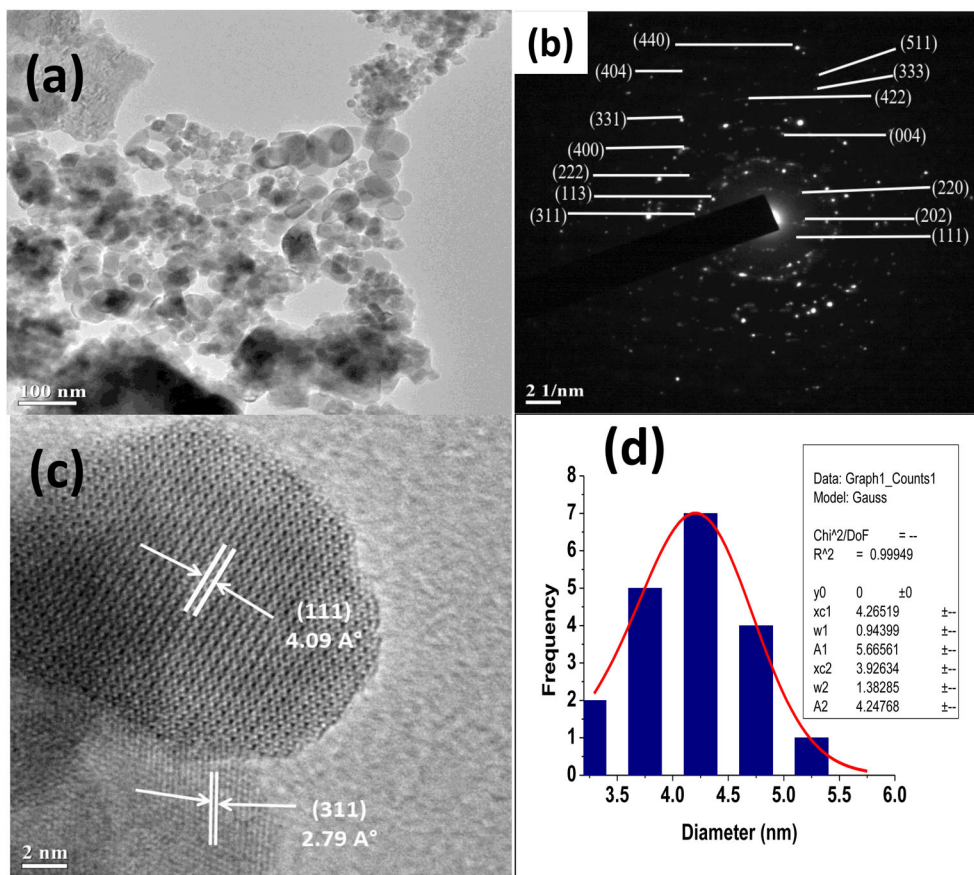**Figure 2.** EDX image of the CuFe$_2$O$_4$ MNPs.

Figure 3. (a) TEM images, (b) corresponding SAED pattern of the nanoparticles, (c) HR-TEM image of selected region of CuFe$_2$O$_4$ MNPs and (d) size distribution of the CuFe$_2$O$_4$ MNPs.
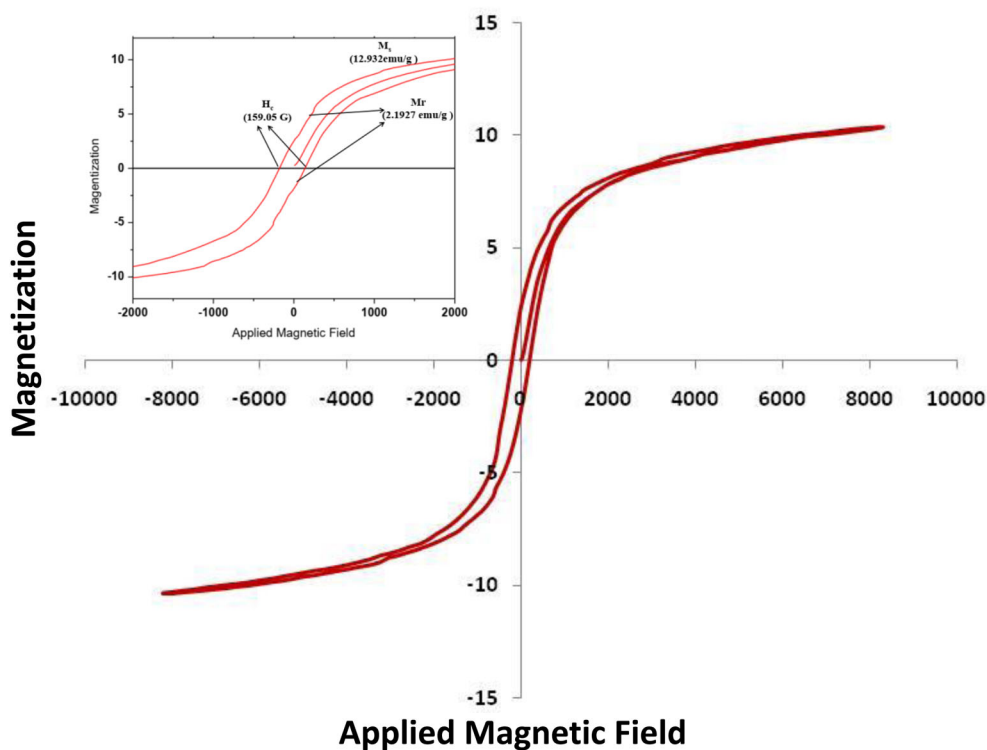
**Figure 4.** VSM of CuFe$_2$O$_4$ MNPs (inset shows the enlarged VSM plot).

different directions. From the size distribution histogram as determined by a large number of particles of TEM image the size of the nanoparticle was 4.27 nm (Figure 3(d)).

By using a vibrating sample magnetometer (VSM), magnetic study was carried out at room temperature for the biogenic CuFe$_2$O$_4$ MNPs (Figure 4). An S-type plot was shown by the M-H curve. The coercivity (Hci) of 159.05 G, magnetization (Ms) 12.932 emu/g and retentivity (Mr) 2.1927 emu/g were found from the VSM analysis. These data confirmed that the nanoparticles were ferromagnetic. This ferromagnetic property of the nanoparticles helped in the easy recyclability and reuse of the catalyst several times. The inset in Figure 4 shows the enlarged hysteresis loop of the CuFe$_2$O$_4$ MNPs.

3.2. Synthesis of phenols by using CuFe$_2$O$_4$ MNPs

The synthesized nanoparticles were used for *ipso*-hydroxylation of aryl boronic acid to phenols. Arylboronic acids react in the presence of water and molecular oxygen to give phenols in good to excellent yield, without a toxic oxidizing agent or base (Scheme 1).

Our first aim was to optimize the amount of catalyst and the source of -OH under different conditions so that it can be applied to a variety of substrates. The optimization was done using 4-methoxy phenyl boronic acid as the model substrate (Table 2).
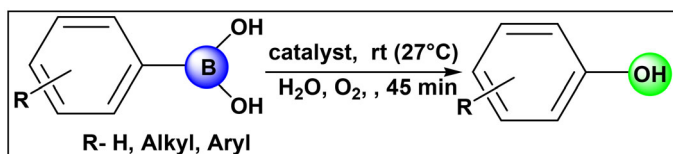
Scheme 1. General scheme of *ipso*-hydroxylation of aryl boronic acids to phenols.

Table 2. Optimization of the catalyst and reaction conditions.[a]

Entry	Catalyst (mol%)	Reaction condition (rt)	Time (h)	Yield (%)[b]
1	1	O_2	5	60
2	3	O_2	4	70
3	6	O_2	40 min	95
4	6	N_2	20	85
5	6	Air	10	88

[a]Reaction conditions: 4-methoxy phenyl boronic acid (0.20 mmol), 3 mL water, rt (27 °C).
[b]Isolated yields.

Only 6 mol% of the catalyst was necessary for complete conversion to 4-methoxy phenol. Moreover, the reaction proceeded smoothly with the use of O_2 and H_2O within a short reaction time. The reaction required longer time when N_2 gas was used (Table 2, entry 4). By using only H_2O, isolated product was obtained but the reaction took about 10 h for completion (Table 2, entry 5). Thus, it was confirmed that both molecular O_2 and H_2O was necessary for the progress of the reaction.

After identification of the proper optimized conditions 16 different phenols were synthesized from aryl boronic acids and aryl boronic esters (Table 3). Both electron-withdrawing and electron-donating groups and the position of the substituent had little effect on the reaction conditions. The heteroarylboronic acids also gave excellent yields.
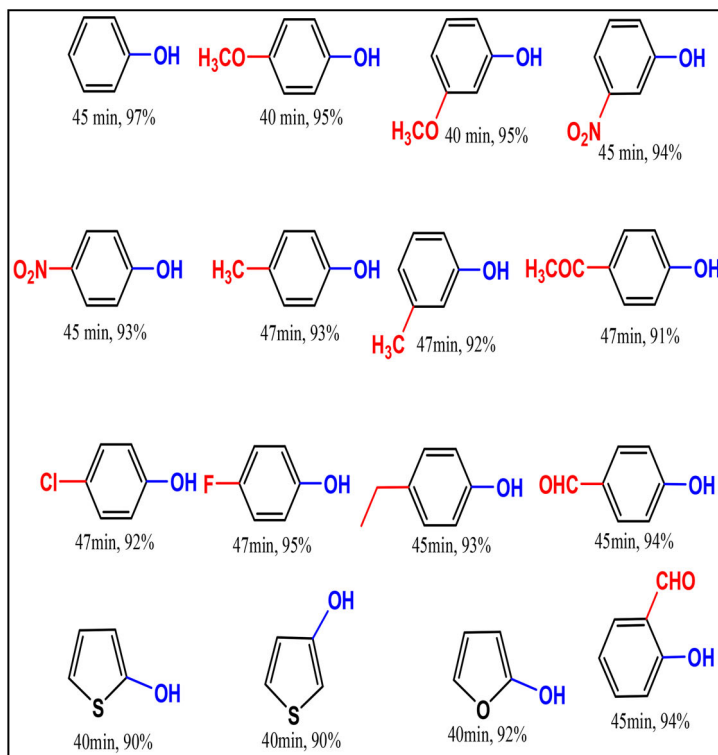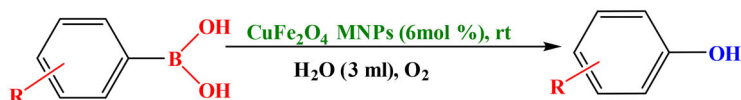
We extended our study to *ipso*-hydroxylation of boronic esters (Table 4). Heteroarylboronic acid esters were conveniently converted to their corresponding phenols and alcohol in a short reaction time.

The *ipso*-hydroxylation of arylboronic acid to phenol was compared with other reported catalysts (Table 5). Our catalyst was superior and greener than other reported catalysts.

3.3. Mechanism

The exact mechanism for the formation of phenols by *ipso*-hydroxylation is unknown. Based on the previously reported mechanisms using a solid support in organic synthesis we provide a brief mechanistic pathway [45, 46] (Figure 5). When the reaction was carried out in the presence of H_2O, it required longer reaction time (Table 2, entry 5), confirming that O_2 was necessary for the smooth and fast progress of the reaction. Therefore we tried to provide a brief mechanistic pathway using H_2O and molecular O_2 as the green oxidizing agent in the reaction.
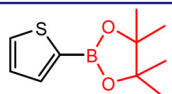
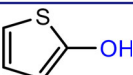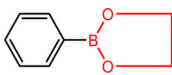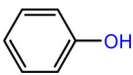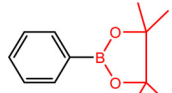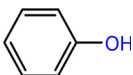Initially, the boron atom adopts sp^2 hybridization in organoboronic acids [47] and gets activated by coordinating on the surface of the $CuFe_2O_4$ as Lewis acidic sites. The boron group thus changes from being a low reactive electrophile into a moderately

Table 3. CuFe$_2$O$_4$ MNPs catalyzed *ipso*-hydroxylation of aryl boronic acids.[a]

45 min, 97%   40 min, 95%   H$_3$CO 40 min, 95%   O$_2$N 45 min, 94%

45 min, 93%   47min, 93%   H$_3$C 47min, 92%   47min, 91%

47min, 92%   47min, 95%   45min, 93%   45min, 94%

40min, 90%   40min, 90%   40min, 92%   45min, 94%

[a]Reaction conditions: arylboronic acid (0.20 mmol), CuFe$_2$O$_4$ MNPs (6 mol%) in 3 mL water and molecular O$_2$, rt (27 °C).
[b]Isolated yields.

Table 4. *Ipso*-hydroxylation of boronic esters.[a]

S. No.	Substrate	Product	Time (min)	Yield (%)[b]
1.			40	95
2.			45	90
3.			50	90

[a]Reaction conditions: arylboronic ester (0.20 mmol), CuFe$_2$O$_4$MNPs (6 mol%) in 3 mL water and molecular O$_2$, rt (27 °C).
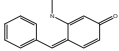[b]Isolated yields.

Table 5. Comparison of ipso-hydroxylation with reported catalysts.

Catalyst	Time (h)	Catalyst (mol%)	Yield (%)	Recycle	Reference
CuSO$_4$	3	10	90	No	[24]
Photocatalyst α-Fe$_2$O$_3$	5	25	90	No	[38]
NH$_2$OH	26	150	68	No	[13]
Cu$_2$O nanoparticles	5	34	95	Yes	[39]
UNLPF-12	8	0.5	93	No	[40]
(structure)	42	1	97	No	[41]
Cu NPs-EA	8	16.7	91	Yes	[42]
Light	8	—	92	No	[43]
Photo organocatalytic	72	20	76	No	[44]
CuFe$_2$O$_4$ MNPs	45 min	6	97	Yes	This work
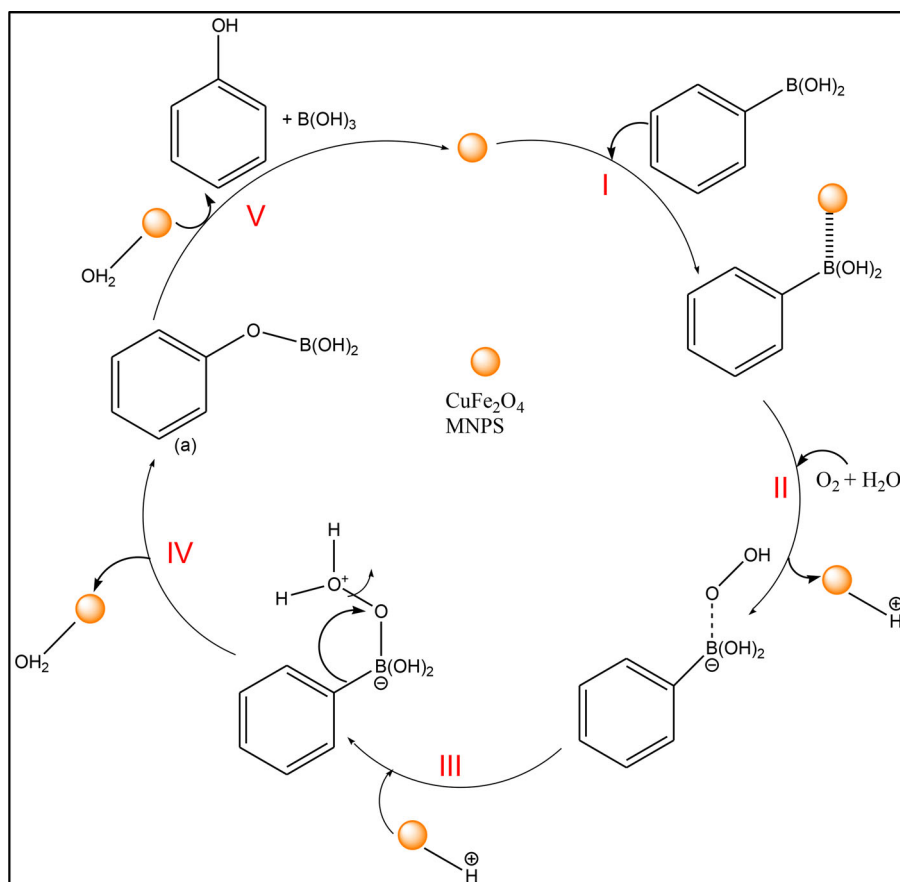
Figure 5. Proposed mechanism for the formation of phenols by *ipso*-hydroxylation.

reactive electrophile due to its coordination to the acidic sites on the surface of the catalyst. The addition of O$_2$+H$_2$O generates a tetravalent boron "ate" complex and induces rehybridization to form sp^3 boron in the –O$_2$H oxidative pathway. Due to the high electron density on boron and increased steric crowding in the "ate" complex the C-B bond dissociates and subsequent aryl migration to the adjacent acceptor oxygen with retention of configuration takes place with elimination of H$_2$O. This H$_2$O
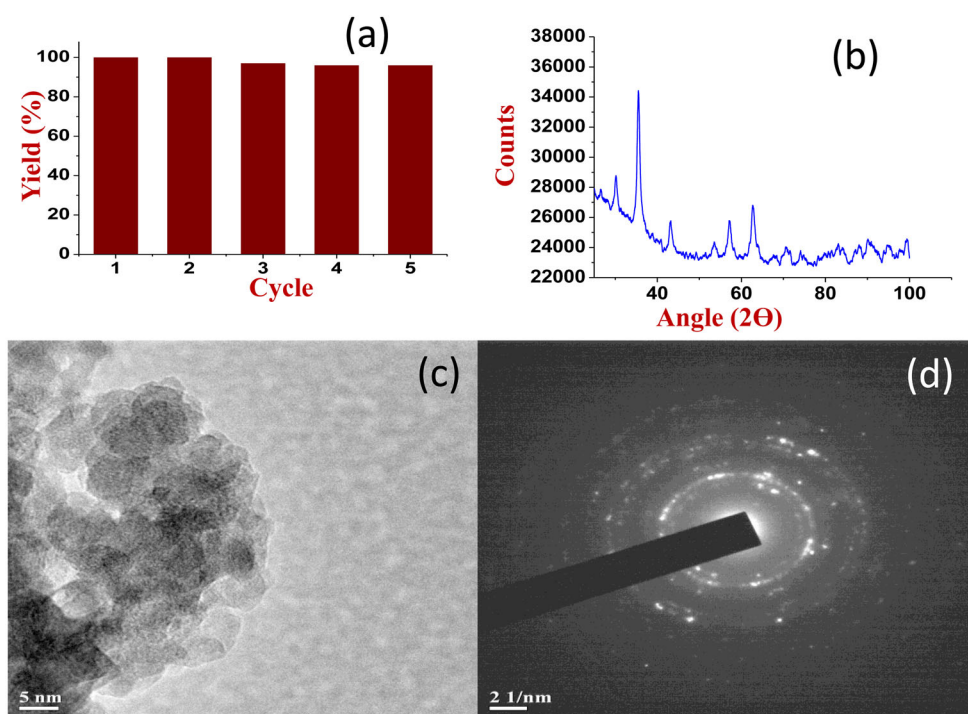
Figure 6. (a) Recyclability of CuFe$_2$O$_4$ MNPs. (b) XRD of the recycled catalyst taken after the fifth cycle. (c) TEM image of recyclable CuFe$_2$O$_4$ MNP's. (d) SAED pattern (fifth cycle).

molecule than approaches the intermediate (a) and hydrolysis step occurs to form the final phenol product.

3.4. Recyclability

Recyclability is a major advantage of a heterogeneous catalyst. The prepared catalyst was easily recyclable with the help of an external magnet without filtration or tedious workup (Figure 6). The catalyst was easily recyclable up to the fifth cycle without significant loss in catalytic activity. The sharp XRD diffraction peaks taken after the fifth cycle depict that the crystalline nature of the MNPs was retained in the recycled catalyst. The TEM image (Figure 6(c)) taken after the fifth cycle showed no change in the morphology, and the bright rings in the SAED pattern (Figure 6(d)) of the recycled catalyst also represent the crystallinity of the nanocatalyst. The slight loss in catalytic activity after the fifth cycle might be due to loss of the nanoparticles due to the recycling process.

4. Conclusion

An environmentally friendly, biogenic route has been designed for the synthesis of CuFe$_2$O$_4$ MNPs with 4.27 nm size using the flowers of *Lantana camara*. The catalyst worked without the use of a toxic oxidizing agent such as H$_2$O$_2$ or harsh reaction conditions. Only water and molecular O$_2$ were necessary for the synthesis of phenols from

arylboronic acid at room temperature within a short reaction time. The catalyst proved to be superior compared to reported catalysts. This is a green route for the synthesis of phenols with high yield products both from environmental and economic point of view.

Acknowledgement

Disclosure statement

No potential conflict of interest was reported by the authors.

References

[1]   S. Nandi, M. Vracko, M.C. Bagchi. *Chem. Biol. Drug. Des.*, **70**, 424 (2007).
[2]   B. Badhani, N. Sharma, R. Kakkar. *RSC Adv.*, **5**, 27540 (2015).
[3]   S.P. Quideau, D. Deffieux, C. Douat-Casassus, L. Pouységu. *Angew. Chem. Int. Ed. Engl.*, **50**, 586 (2011).
[4]   P. Williams, A. Sorribas, M.J.R. Howes. *Nat. Prod. Rep.*, **28**, 48 (2011).
[5]   J.E.O. Connell, P.F. Fox. *Int. Dairy J.*, **11**, 103 (2001).
[6]   N. Balasundram, K. Sundram, S. Samman. *Food Chem.*, **99**, 191 (2006).
[7]   R.K. Choudhary, P.L. Swarnkar. *Nat. Prod. Res.*, **25**, 1101 (2011).
[8]   L.G. Ranilla, Y.I. Kwon, E. Apostolidis, K. Shetty. *Bioresour. Technol.*, **101**, 4676 (2010).
[9]   C. Yu, G.S. Chen, C.W. Huang, J.W. Chern. *Org. Lett.*, **14**, 3688 (2012).
[10]   R.E. Maleczka, F. Shi, D. Holmes, M.R. Smith. *J. Am. Chem. Soc.*, **125**, 7792 (2003).
[11]   D.S. Chen, J.M. Huang. *Synlett.*, **24**, 499 (2013).
[12]   P. Fontani, B. Carboni, M. Vaultier, G. Maas. *Synthesis*, **1991**, 605 (1991).
[13]   E. Kianmehr, M. Yahyaee, K. Tabatabai. *Tetrahedron Lett.*, **48**, 2713 (2007).
[14]   S.M. Guo, L. Lu, H. Cai. *Synlett.*, **24**, 1712 (2013).
[15]   C. Zhu, R. Wang, J.R. Falck. *Org. Lett.*, **14**, 3494 (2012).
[16]   T. Begum, A. Gogoi, P.K. Gogoi, U. Bora. *Tetrahedron Lett.*, **56**, 95 (2015).
[17]   A. Gogoi, U. Bora. *Tetrahedron Lett.*, **54**, 1821 (2013).
[18]   N. Mulakayala, K.M. Ismail, R.K. Kumar, B. Rapolu, P. Kandagatla, S. Rao, M.P. Oruganti. *Tetrahedron Lett.*, **53**, 6004 (2012).
[19]   G.K.S. Prakash, S. Chacko, C. Panja, T.E. Thomas, L. Gurung, G. Rasul, T. Mathew, G.A. Olah. *Adv. Synth. Catal.*, **351**, 1567 (2009).
[20]   C.J. Li. *Chem. Rev.*, **105**, 3095 (2005).
[21]   P.R. Boruah, A.A. Ali, M. Chetia, B. Saikia, D. Sarma. *Chem. Commun. (Camb.)*, **51**, 11489 (2015).
[22]   K. Yang, Z. Li, Z. Wang, Z. Yao, S. Jiang. *Org. Lett.*, **13**, 4340 (2011).
[23]   K. Inamoto, K. Nozawa, M. Yonemoto, Y. Kondo. *Chem. Commun. (Camb.)*, **47**, 11775 (2011).
[24]   J. Xu, X. Wang, C. Shao, D. Su, G. Cheng, Y. Hu. *Org. Lett.*, **12**, 1964 (2010).
[25]   D. Yang, B. An, W. Wei, M. Jiang, J. You, H. Wang. *Tetrahedron*, **70**, 3630 (2014).
[26]   R. Chutia, B. Chetia. *J. Chem. Sci.*, **131**, 48 (2019).
[27]   J.M. Watt, M.G. Breyer-Brandwijk. *The Medicinal and Poisonous Plants of Southern and Eastern Africa*, 2nd Edn, pp 1049–1050, Livingstone, London (1962).

[28] O.B. Bever. *Medicinal Plants in West Africa*, p. 118, Cambridge University Press, London (1982).
[29] S. Begum, S.Q. Zehra, B.S. Siddiqui. *Chem. Pharm. Bull.*, **56**, 1317 (2008).
[30] D.K. Verma, S.K. Singh, V. Tripathi. *Indian Drugs*, **34**, 32 (1997).
[31] D. Bhakta, D. Ganjewala. *J. Sci. Res.*, **1**, 363 (2009).
[32] K. Kombaiah, J.J. Vijaya, L.J. Kennedy, M. Bououdina, B. Al-Najar. *J. Phys. Chem. Solids*, **115**, 162 (2018).
[33] A.A. Hunaiti, N.A. Said, L. Halawani, M.A. Haija, R. Baqaien, D. Taher. *Arab. J. Chem.*, **13**, 4945 (2020).
[34] B.S. Surendra, M. Veerabhdraswamy, K.S. Anantharaju, H.P. Nagaswarupa, S.C. Prashantha. *J. Nanostruct. Chem.*, **8**, 45 (2018).
[35] A. Ramazania, S.T. Fardood, Z. Hosseinzadeh, F. Sadri, S.W. Joo. *Iran. J. Catal.*, **7**, 181 (2017).
[36] R. Chutia, B. Chetia. *Tetrahedron Lett.*, **58**, 3864 (2017).
[37] R. Chutia, B. Chetia. *New J. Chem.*, **42**, 15200 (2018).
[38] S.D. Sawant, A.D. Hudwekar, K.A.A. Kumar, V. Venkateswarlu, P.P. Singh, R.A. Vishwakarma. *Tetrahedron Lett.*, **55**, 811 (2014).
[39] R. Borah, E. Saikia, S.J. Bora, B. Chetia. *RSC Adv.*, **6**, 100443 (2016).
[40] J.A. Johnson, J. Luo, X. Zhang, Y.-S. Chen, M.D. Morton, E. Echeverría, F.E. Torres, J. Zhang. *ACS Catal.*, **5**, 5283 (2015).
[41] H.Y. Xie, L.S. Han, S. Huang, X. Lei, Y. Cheng, W. Zhao, H. Sun, X. Wen, Q.L. Xu. *J. Org. Chem.*, **82**, 5236 (2017).
[42] A. Affrose, I.A. Azath, A. Dhakshinamoorthy, K. Pitchumani. *J. Mol. Catal. A: Chem.*, **395**, 500 (2014).
[43] M. Jiang, Y. Li, H. Yang, R. Zong, Y. Jin, H. Fu. *RSC Adv.*, **4**, 12977 (2014).
[44] I.K. Sideri, E. Voutyritsa, C.G. Kokotos. *Synlett.*, **29**, 1324 (2018).
[45] A. Mahanta, P. Adhikari, U. Bora, A.J. Thakur. *Tetrahedron Lett.*, **56**, 1780 (2015).
[46] X. Yang, X. Jiang, W. Wang, Q. Yang, Y. Ma, K. Wang. *RSC Adv.*, **9**, 34529 (2019).
[47] C. Zhu, J.R. Falck. *Adv. Synth. Catal.*, **356**, 2395 (2014).